Analyzing powers for elastic and inelastic scattering of polarized ^{6}Li from ^{9}Be at 32 MeV

E. L. Reber, K. W. Kemper, P. L. Kerr, A. J. Mendez, E. G. Myers, and B. G. Schmidt
Department of Physics, Florida State University, Tallahassee, Florida 32306

V. Hnizdo
Department of Physics and Schonland Research Centre for Nuclear Sciences, University of the Witwatersrand, Johannesburg, 2050 South Africa

(Received 27 January 1993)

Vector and tensor analyzing powers (iT_{11}, $^TT_{20}$, T_{20}, and T_{22}) for the ^{9}Be($^6\vec{\text{Li}}$,^{6}Li)^{9}Be elastic scattering and inelastic scattering leading to the $5/2^-$ (2.43 MeV) excited state in ^{9}Be are presented for a $^6\vec{\text{Li}}$ bombarding energy of 32 MeV over the c.m. angular range 13°–87°. The results of coupled-channels calculations show that the relatively large observed values of the vector analyzing power iT_{11} for the inelastic scattering can only be accounted for by an explicit spin-orbit term in the optical potential. For the elastic scattering, the vector analyzing power and the relatively small tensor analyzing powers are described reasonably well by coupled-channels calculations with no explicit spin-orbit or tensor terms in the interaction, and provide a severe constraint on the coupled-channels calculations, with a preference for an optical potential with a double-folded rather than a Woods-Saxon real part.

PACS number(s): 24.70.+s, 24.10.−i

I. INTRODUCTION

The larger than expected vector analyzing powers that occur in elastic scattering of ^{6}Li projectiles [1] have been shown [2] to arise from virtual excitation of the ^{6}Li nucleus in the scattering process. Channel coupling effects thus generate dynamically effective spin-dependent interactions, which makes it difficult to learn about the static spin-orbit interaction for heavy ions from the observed vector analyzing powers.

A study by Van Verst *et al.* [3] of the inelastic scattering of polarized ^{6}Li by ^{12}C to its first excited 2^+ state at 4.44 MeV showed the vector analyzing power to be much larger than could be produced by any reasonable coupled-channels calculation, and that these data were quite sensitive to the presence of a static spin-orbit potential. Inelastic-scattering data for $^6\vec{\text{Li}} + {}^{26}$Mg,^{120}Sn [4, 5] also display vector analyzing powers that are larger than those produced by coupled-channels calculations that reproduce the vector analyzing powers for elastic scattering.

In the present work, vector and tensor analyzing powers are reported for the scattering of polarized ^{6}Li by ^{9}Be. The target ^{9}Be was chosen because of the large cross section for the inelastic scattering to its second excited state at 2.43 MeV [6]. An analysis of the data is carried out through coupled-channels calculations that employ an optical potential with a double-folded real part for the ^{6}Li-^{9}Be interaction. The present analysis confirms the need for an explicit (static) spin-orbit term in the optical potential to account for the magnitude of the observed inelastic-scattering vector analyzing powers, and shows that the measured tensor analyzing powers provide a severe constraint on the coupled-channels calculations.

II. EXPERIMENTAL PROCEDURE

A beam of polarized ^{6}Li ions, produced with the Florida State University (FSU) optically pumped polarized Li ion source, was accelerated by the FSU FN Tandem Van de Graaff to 32 MeV and was scattered from a self-supporting ^{9}Be target of thickness 200 μg/cm^2. The detection system employed four ΔE-E telescopes to identify the reaction products. Two telescopes were arranged symmetrically on each side of the beam axis. The polarization of the ^{6}Li beam was monitored using a helium-filled polarimeter that followed the main scattering chamber. The beam energy was decreased to 15.5 MeV at the center of the polarimeter target volume by passing it through Al foils before it entered the polarimeter, where detectors placed at $\theta_{\text{lab}} = \pm 15°$ monitored the reaction ^{4}He($^6\vec{\text{Li}}$, α)^{6}Li. This reaction was used because of its large cross section [7] and vector analyzing powers [8] at 15.5 MeV. Recent work [9] has shown that, at this angle, the tensor analyzing powers are large enough to serve as a beam polarization monitor.

The three magnetic substates of the $^6\vec{\text{Li}}^{3+}$ are $m_I = +1$, 0, and −1. The beam polarization states corresponding to populating these substates will be referred to as N_+, N_0, and N_-, respectively, and an unpolarized beam will be referred to as the "off" polarization state. During data acquisition the polarization state of the beam was automatically cycled through the off, N_+, N_0, and N_-

states, spending approximately 2 min in each state.

The typical $^6Li^{3+}$ beam current on target was 30–50 electrical nA. The beam contained vector and tensor polarization components in all three spin states. Typical on target beam populations can be seen in Table I. The on target beam vector polarization for the N_+ state was determined to be [9] $t_{10} = 1.05 \pm 0.05$, and the tensor polarization for the N_0 state was determined to be [9] $t_{20} = -0.87 \pm 0.05$. The Madison convention [10] is used in this work for the description of polarization observables. When, however, quantities relating to a frame in which the spin quantization axis is normal to the scattering plane, the "transverse" frame is employed, they are denoted by a left superscript T.

The vector and tensor analyzing powers (VAP's and TAP's) were both measured in the c.m. angular range from 13°–87° with detectors placed symmetrically to the left and right of the beam. The size of the error bars in the figures show the statistical uncertainty in the analyzing powers. The VAP's were measured with the polarization axis normal to the scattering plane, and were determined using the relation

$$iT_{11}(\theta) = \frac{L - R}{2\sqrt{2}\, t_{10}} , \tag{1}$$

where $L = L_{\rm pol}/L_{\rm off}$ and $R = R_{\rm pol}/R_{\rm off}$. The quantities $L_{\rm pol}$ ($R_{\rm pol}$) and $L_{\rm off}$ ($R_{\rm off}$) represent the number of particles accumulated in the detector to the left (right) of the beam when the ^{6}Li was polarized and unpolarized, respectively. The VAP's were also computed for each left and right detector separately by using the N_+ and N_- states to make certain that no change in the efficiency of the detector pair occurred during the runs. The TAP's were determined from the results using the relation

$$^TT_{20}(\theta) = \frac{L + R - 2}{2\, t_{20}} , \tag{2}$$

for the polarization axis aligned normal to the scattering plane, and

$$T_{20}(\theta) = \frac{L + R - 2}{2\, t_{20}} , \tag{3}$$

for the polarization axis parallel to the beam axis. The analyzing power T_{22} was deduced from the measured quantities $^TT_{20}$ and T_{20} using the relation

$$T_{22}(\theta) = -\sqrt{\tfrac{1}{6}}\, T_{20}(\theta) - \sqrt{\tfrac{2}{3}}\, {}^TT_{20}(\theta) . \tag{4}$$

TABLE I. Typical on target population distributions and $^6Li^{3+}$ beam polarizations for each run state during a typical cycle.

	Off state	N_+ state	N_0 state	N_- state
$m_I = +1$	33.3%	86.8%	18.9%	2.1%
$m_I = 0$	33.3%	11.6%	74.4%	13.3%
$m_I = -1$	33.3%	1.6%	6.6%	84.6%
t_{10}	0.000	1.045	0.151	-1.010
t_{20}	0.000	0.461	-0.871	0.425

III. ANALYSIS

The present analysis employed the double-folding model [11] for the optical potential describing the ^{6}Li-^{9}Be interaction. The real part of the optical potential was obtained by folding the nucleon densities of ^{6}Li and ^{9}Be with the M3Y effective nucleon-nucleon interaction of Bertsch *et al.* (the S=T=0 term only) [12] supplemented with a term approximating single-nucleon knockout exchange [13]. The imaginary part of the potential had the standard Woods-Saxon shape. The optical potential had thus only four adjustable parameters: the renormalization factor of the double-folded (DF) real part plus the three parameters of the Woods-Saxon (WS) imaginary part.

Spin-dependent and deformation-dependent (tensor) terms of the ^{6}Li-^{9}Be interaction, which generate vector and tensor analyzing powers, were obtained dynamically by performing coupled-channels (CC) calculations that involved the excitation and reorientation of the projectile nucleus ^{6}Li. It is now well established that such coupling effects produce vector and tensor analyzing powers that contribute dominantly to these observables in elastic scattering of polarized ^{6}Li nuclei, removing the need for an explicit spin-orbit term in the optical potential [14]. The coupling potentials employed in the CC calculations had, like the diagonal potential, a DF real part and a WS imaginary part. Similar coupling potentials were used in CC calculations involving the excitation of the target nucleus ^{9}Be to its first excited state. The need for an explicit (static) spin-orbit term in the optical potential was also investigated, in particular for the description of the observed analyzing powers for the inelastic scattering leading to the $5/2^-$ (2.43 MeV) state in ^{9}Be, as previous work indicated that the dynamic effects involving the excitation of ^{6}Li were insufficient to account for the magnitude of the observed analyzing powers for inelastic scattering leading to the excitation of the target nuclei ^{12}C [3] and ^{26}Mg [4].

The nucleon density of ^{6}Li was obtained from the measured charge density of Suelzle, Yearian, and Crannel [15] by assuming that the proton and neutron distributions were the same. The proton part of the density of the ^{9}Be nucleus was taken from electron scattering work [16], and the neutron part was adjusted so that the difference between the neutron and proton rms radii, after a deconvolution of the proton size, was 0.38 fm (method B of Ref. [17]). The parameters of the densities used are given in Table II. The parameters of the optical potential, obtained by fitting the angular distribution for the elastic scattering of ^{6}Li from ^{9}Be at $E_{\rm lab} = 32$ MeV [6], are given in Table III. Note that the renormalization of the DF real part of the potential by a factor $N = 0.8$, which was required for the best fit, is not as dramatic as that usually needed for the description of elastic scattering of the nuclei ^{6}Li and ^{9}Be in the double-folding model [17, 18].

The coupling potentials, required in the CC calculations of the excitation and reorientation of the nucleus ^{6}Li, and for the inelastic scattering to the $5/2^-$ (2.43 MeV) state in ^{9}Be, were obtained by using the following

TABLE II. Parameters of the projectile and target nucleon densities. The densities have the form $\rho(r) = (A + BC^2r^2)e^{-C^2r^2} + (D + EF^2r^2)e^{-F^2r^2}$. The proton size is unfolded from these densities in a momentum-space evaluation of the double-folded potential.

	A (fm^{-3})	B (fm^{-3})	C (fm^{-1})	D (fm^{-3})	E (fm^{-3})	F (fm^{-1})
^{6}Li	0.1666	0.0	0.5380	−0.0114	0.0074	0.3840
^{9}Be	0.0651	0.0398	0.5580	0.0544	0.0332	0.4878

simple form for the radial part of the transition density of the excited (reorientated) nucleus:

$$\rho_2(r) = -\delta_2 \frac{d\rho(r)}{dr}. \quad (5)$$

Here $\rho(r)$ is the ground-state (monopole) density of the nucleus concerned, and δ_2 is an intrinsic quadrupole deformation length. Only quadrupole ($\ell = 2$) angular momentum transfers were included in the calculations. The imaginary part of the coupling potentials had the standard derivative WS form, with the same deformation length as that used in the DF real part. The rotational model was used for the calculation of the excitation and reorientation coupling strengths, assuming a bandhead K equal to the spin of the ground state of the nucleus concerned.

Similar CC calculations, employing DF diagonal and coupling potentials and also involving the nuclei ^{6}Li and ^{9}Be, are described in more detail in Refs. [19] and [20]. The calculations reported here were performed using the CC code CHUCK [21].

A. Elastic-scattering analyzing powers

The optical potential obtained by fitting the angular distribution for ^{6}Li + ^{9}Be elastic scattering was the starting point of CC calculations in which the first excited state of ^{6}Li (3^+, 2.18 MeV) was coupled to its ground 1^+ state and both the ground and the excited state of ^{6}Li were coupled to themselves (these are the so-called reorientation couplings). The intrinsic deformation lengths required in a double-folding description of inelastic ^{6}Li scattering from the nuclei ^{12}C and ^{16}O are in the range $|\delta_2| = 1.89$–2.34 fm [3], but for the system ^{6}Li + ^{9}Be no experimental data are yet available for the excitation of the nucleus ^{6}Li. In view of this, the deformation length of the $1^+ \rightarrow 3^+$ transition in ^{6}Li was fixed so that the magnitude of the measured elastic-scattering vector analyzing power was reproduced at its first negative minimum at $\theta_{\mathrm{c.m.}} \simeq 38°$. This required the value $\delta_2 = -1.82$ fm. The negative sign of δ_2 was chosen in accordance with the results of a previous CC analysis of ^{6}Li scattering [19]. The reorientation deformation lengths were set at a half of the value for the $1^+ \rightarrow 3^+$ transition, following the procedure adopted in Refs. [3] and [19]. The optical potential parameters were adjusted for the explicit treatment of the coupling effects by increasing the renormalization factor of the DF real part of the potential to $N = 0.9$, together with a change in the strength of the imaginary potential (see Table III).

The results of these two-channel calculations are shown by solid lines in Fig. 1. The main features of the observed analyzing powers iT_{11}, $^7T_{20}$, T_{20}, and T_{22} are seen to be accounted for, with no apparent need for any explicit spin-orbit term in the optical potential. The effects of the coupling to higher excited ($T = 0$) states in ^{6}Li were investigated by including the 2^+ (4.31 MeV) state of ^{6}Li in a coupling scheme in which all the quadrupole transitions between the 1^+, 3^+ and 2^+ states, together with quadrupole reorientations of these states were considered. The same value of intrinsic δ_2 as in the two-channel calculation was used (with a value of $\delta_2/2$ for reorientation). The main effect of the inclusion of the 2^+ state is a de-

TABLE III. Optical potentials and deformation lengths. The optical potential has a double-folded real part, renormalized by a factor N, and a Woods-Saxon imaginary part with strength, radius parameter, and diffuseness W, r_I, and a_I, respectively. The parameters labeled SO are those of a real Thomas spin-orbit potential.

	N	W (MeV)	r_I[a] (fm)	a_I (fm)	δ_2[b] (fm)	V_{SO}[c] (MeV)	r_{SO}[a] (fm)	a_{SO} (fm)
OM[d]	0.8	11.55	2.30	0.655	0	0		
CC[e]	0.9	12.55	2.30	0.655	−1.82	0		
CC + SO[f]	0.9	12.55	2.30	0.655	1.58	10	1.3	0.6

[a] $R = r A_t^{1/3}$.

[b] Reduced by a factor 1/2 in reorientation couplings.

[c] Explicit factor $(\hbar/m_\pi c)^2$ and operator $\mathbf{l} \cdot \mathbf{s}$ assumed in the spin-orbit potential.

[d] Optical model calculation with no coupling effects.

[e] Coupled-channels calculation: ^{6}Li($1^+ \rightarrow 3^+$, and reorientation).

[f] Coupled-channels calculation: ^{9}Be($0^+ \rightarrow 2^+$).

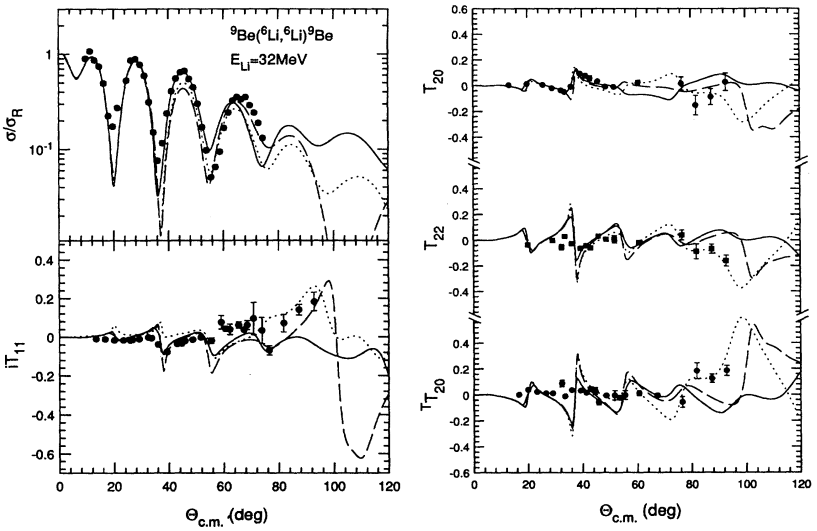

FIG. 1. Differential cross sections [6] and analyzing powers for elastic scattering of ^{6}Li + ^{9}Be at E_{lab} = 32 MeV. The solid line is a two-channel calculation with no spin-orbit potential, involving the excitation of the 3^+ excited state of ^{6}Li and reorientation effects; the dashed line is a three-channel calculation with no spin-orbit potential, involving also the excitation of the $5/2^-$ state (treated as a 2^+ state) of ^{9}Be; the dotted line is a three-channel calculation involving the 3^+ state of ^{6}Li and the $5/2^-$ state (treated as a 2^+ state) of ^{9}Be, with a spin-orbit potential. The potential parameters used are summarized in Table III.

crease in the amplitude of the oscillations of the iT_{11} analyzing power, while the effect on $^TT_{20}$ is opposite: The amplitude of the oscillations there increased appreciably. Both effects worsened the agreement between theory and data. It was felt that CC calculations involving more than the first excited state of ^{6}Li, and thus also more parameters (such as the coupling strengths), would have to provide an appreciable improvement in the description of the data in order to be meaningful and justifiable. In the present work this does not seem to be the case for the system studied, in contrast to findings of analyses of polarized ^{6}Li scattering from heavier targets [4, 22].

The iT_{11}, $^TT_{20}$, T_{20}, and T_{22} analyzing powers were also calculated in the two-channel coupling scheme using the phenomenological WS potential of Ref. [6] for both the real and imaginary parts of the optical potential. The results of these calculations were found to be less satisfactory than those with the DF potential as, in addition to the coupling effects involving the first excited state of ^{6}Li, an explicit spin-orbit potential with both real and imaginary parts was required to produce an iT_{11} analyzing power with a negative minimum at $\theta_{c.m.} \simeq 38°$, which is seen in the experimental data. Moreover, the tensor analyzing power $^TT_{20}$ that resulted in these calculations oscillated with a much larger amplitude than that of the experimental $^TT_{20}$. For this reason, optical potentials with a real WS part were not used further in the analysis.

B. Inelastic-scattering analyzing powers

The measured analyzing powers iT_{11}, $^TT_{20}$, T_{20}, and T_{22} for the inelastic scattering of ^{6}Li leading to the $5/2^-$ (2.43 MeV) excited state in ^{9}Be were first attempted to be analyzed in three-channel calculations in which, apart from the $1^+ \rightarrow 3^+$ transition and reorientation effects in ^{6}Li, the transition between the ground state and the 2.43 MeV excited state of ^{9}Be was also included. To reduce the excessive number of subchannels that would be required in such calculations because of the ground-state spin 3/2 of ^{9}Be, the problem was simplified by treating the excitation of ^{9}Be as a $0^+ \rightarrow 2^+$ transition, with no reorientation of the 2^+ state. Apart from a rescaling of the intrinsic deformation length appropriate for this transition, viz.,

$$\delta_2(0^+ \rightarrow 2^+) \approx \left\langle \frac{3}{2}\, 2\, \frac{3}{2}\, 0 \mid \frac{5}{2}\, \frac{3}{2} \right\rangle \delta_2 \left(\frac{3}{2}^- \rightarrow \frac{5}{2}^- \right)$$

$$= 0.7174\, \delta_2 \left(\frac{3}{2}^- \rightarrow \frac{5}{2}^- \right), \qquad (6)$$

and the neglect of reorientation effects, it was felt that this simplification was adequate for our purpose. The value of $\delta_2(0^+ \rightarrow 2^+)$ was adjusted to fit the measured cross section for the inelastic scattering of ^{6}Li leading to the $5/2^-$ state in ^{9}Be [6]. The value $\delta_2(0^+ \rightarrow 2^+) = 1.58$ fm was obtained in this way, which is consistent with the value $\delta_2(3/2^- \rightarrow 5/2^-) = 1.9$ fm obtained in the CC analysis of Ref. [6].

The analyzing powers iT_{11}, $^TT_{20}$, T_{20}, and T_{22} for the inelastic scattering produced in these three-channel calculations are shown in Fig. 2 by dashed lines. They are rather small, and in particular the iT_{11} analyzing power seriously underestimates the magnitude of the experimental quantities. This is in agreement with findings of previous analyses [3, 4] of iT_{11} analyzing powers in inelastic scattering. In view of these results, the inelastic-scattering analyzing powers were analyzed in two-channel calculations that involved only the transition in the target nucleus ^{9}Be, treated again as a $0^+ \rightarrow 2^+$ excitation, but in which an explicit real spin-orbit term for the ^{6}Li projectile was included in the optical potential. The spin-orbit potential had the standard Thomas WS form, whose parameters are given in Table III. The resulting analyzing powers iT_{11}, $^TT_{20}$, T_{20}, and T_{22} for the inelastic scattering are shown as solid lines in Fig. 2. It can be seen that the calculations with the spin-orbit potential result in an analyzing power iT_{11} that accounts for the gross features of the experimental data, but the calcu-

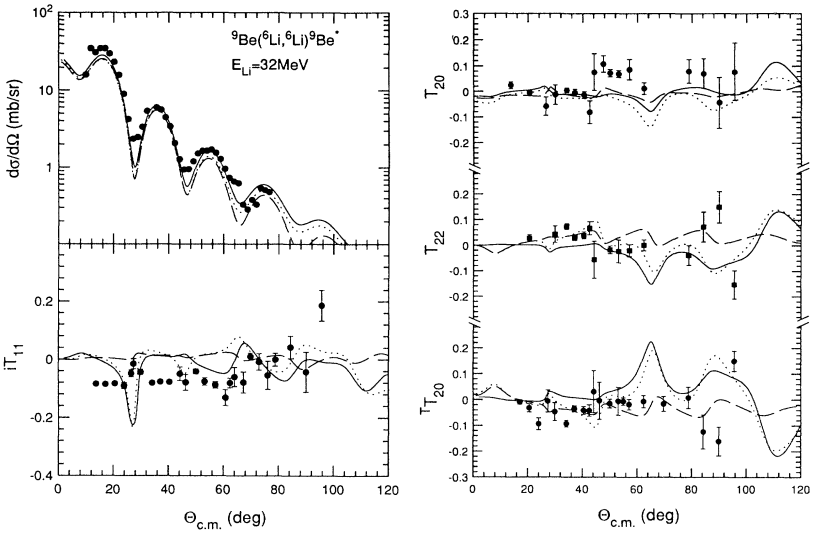

FIG. 2. Differential cross sections [6] and analyzing powers for the inelastic scattering ^{9}Be($^6\vec{\text{Li}}$,^{6}Li)^{9}Be*$(5/2^-)$ at E_{lab} = 32 MeV. The solid line is a two-channel calculation with a spin-orbit potential, involving the excitation of the $5/2^-$ state (treated as a 2^+ state) of ^{9}Be; the dashed line is a three-channel calculation with no spin-orbit potential, involving also the excitation and reorientation of the 3^+ state of ^{6}Li; the dotted line is the same calculation as that of the dashed line, but with a spin-orbit potential. The potential parameters used are summarized in Table III.

lated $^TT_{20}$ for inelastic scattering remains a problem as both to the overall magnitude and sign of the predictions.

The effect of the spin-orbit potential in three-channel calculations was investigated also. These calculations are shown for inelastic-scattering analyzing powers by dotted lines in Fig. 2, where they can be seen not to change significantly the two-channel predictions with the spin-orbit potential. The results of the three-channel calculations for the elastic-scattering powers are shown in Fig. 1 (dashed lines for the calculations without any spin-orbit potential and dotted lines for the calculations with spin-orbit potential), and the inclusion of the spin-orbit potential is seen to improve somewhat the correspondence between the theory and the data at large angles.

IV. CONCLUSION

The present work reports measurements of vector and tensor analyzing powers for $^6\vec{\text{Li}}+^9$Be elastic and inelastic scattering. The inelastic-scattering analyzing powers for the ^{9}Be$(5/2^-$, 2.43 MeV) state are nonzero, with the vector analyzing power iT_{11} for the inelastic scattering being about -0.08. Both the experimental elastic- and inelastic-scattering tensor analyzing powers lack large magnitude and highly oscillatory behavior, which provided a severe restriction on the strength of channel coupling that could be included to describe the scattering process.

No single set of calculations carried out here gave a satisfactory overall representation of the data. The coupled-channels calculations described reasonably well all the observed analyzing powers for the elastic scattering. On the other hand, the coupled-channels calculations failed to account for the analyzing powers of the inelastic scattering. In particular, the inelastic-scattering vector analyzing power iT_{11} was grossly underestimated by the coupled-channels calculations, and a static spin-orbit interaction was required to produce iT_{11} values of the observed magnitude for the inelastic scattering. Thus both elastic- and inelastic-scattering analyzing powers are needed for the determination of the magnitude of the static spin-orbit interaction in the scattering of ^{6}Li projectiles.

An optical potential with a double-folded real part was found to provide a better description of the analyzing powers in the coupled-channels calculations than that obtained with a phenomenological Woods-Saxon potential. However, more microscopic theoretical calculations that include coupling to the nonresonant breakup states [23] in both ^{6}Li and ^{9}Be are needed before the underlying physics contained in the present data set can be extracted.

ACKNOWLEDGMENTS

This work was supported in part by the National Science Foundation and the State of Florida.

[1] W. Weiss, P. Egelhof, K. D. Hildenbrand, D. Kassen, M Makowska-Rzeszutko, D. Fick, H. Ebinghaus, E. Steffens, A. Amakawa, and K.-I. Kubo, Phys. Lett. **61B**, 237 (1976).

[2] H. Niskioka, J. A. Tostevin, R. C. Johnson, and K.-I. Kubo, Nucl. Phys. **A415**, 230 (1984); H. Ohniski, M. Tanifiyi, M. Kanimura, Y. Sakuagi, and M. Yahiro, *ibid.* **A415**, 271 (1984); F. Petrovich, R. J. Philpott, A. W. Carpenter, and J. A. Carr, *ibid.* **A425**, 609 (1984).

[3] S. P. Van Verst, D. P. Sanderson, D. E. Trcka, K.W. Kemper, V. Hnizdo, B. G. Schmidt, and K. R. Chapman, Phys. Rev. C **39**, 853 (1989).

[4] K. Rusek, J. Giroux, H. J. Jänsch, H. Vogt, K. Becker, K. Blatt, A. Gerlach, W. Korsch, H. Leucker, W. Luck, H. Reich, H.-G. Völk, and D. Fick, Nucl. Phys. **A503**, 223 (1989).

[5] K. Becker, K. Blatt, W. Korsch, H. Leucker, W. Luck, H. Reich, H.-G. Völk, D. Fick, K. Rusek, and H. J. Jänsch, Nucl. Phys. **A535**, 189 (1991).

[6] J. Cook and K.W. Kemper, Phys. Rev. C **31**, 1745

(1985).
[7] H. G. Bingham, K. W. Kemper, and N. R. Fletcher, Nucl. Phys. **A175**, 374 (1971).
[8] P. Egelhof, J. Barrette, P. Braun-Munzinger, W. Dreves, C. K. Gelbke, D. Kassen, E. Steffens, W. Weiss, and D. Fick, Phys. Lett. **84B**, 176 (1979).
[9] A. J. Mendez, E. G. Meyers, K. W. Kemper, P. L. Kerr, E. L. Reber, and B. G. Schmidt, Nucl. Instrum. Methods (to be published).
[10] *Polarization Phenomena in Nuclear Reactions*, edited by H.H. Barschall and W. Haeberli (University of Wisconsin Press, Madison, 1971).
[11] G.R. Satchler and W.G. Love, Phys. Rep. **55**, 185 (1979).
[12] G. Bertsch, J. Borysowicz, H. McManus, and W.G. Love, Nucl. Phys. **A284**, 399 (1977).
[13] M. Golin, F. Petrovich, and D. Robson, Phys. Lett. **64B**, 253 (1976).
[14] D. Fick, G. Grawert, and I.M. Turkewicz, Phys. Rep. **214**, 1 (1992).
[15] L.R. Suelzle, M.R. Yearian, and H. Crannel, Phys. Rev. **162**, 992 (1967).
[16] C.W. de Jager, H. de Vries, and C. de Vries, At. Data Nucl. Data Tables **14**, 479 (1974).
[17] G.R. Satchler, Phys. Lett. **83B**, 284 (1979).
[18] G.R. Satchler and W.G. Love, Phys. Lett. **76B**, 23 (1978).
[19] M.F. Vineyard, J. Cook, and K.W. Kemper, Phys. Rev. C **31**, 879 (1985).
[20] V. Hnizdo, J. Szymakowski, K.W. Kemper, and J.D. Fox, Phys. Rev. C **24**, 1495 (1981).
[21] P.D. Kunz, University of Colorado Report (unpublished) with modifications by J.R. Comfort, J. Cook and V. Hnizdo.
[22] Y. Hirabayashi and Y. Sakuragi, Nucl. Phys. **A536**, 375 (1992).
[23] Y. Sakuragi, M. Yahiro, and M. Kamimura, Prog. Theor. Phys. **70**, 1047 (1983); Y. Hirabayashi, Phys. Rev. C **44**, 1581 (1991).